Available online at www.sciencedirect.com
SCIENCE DIRECT
Thin Solid Films 494 (2006) 287 – 290
thin solid films
www.elsevier.com/locate/tsf

Memory effect of sol–gel derived V-doped $SrZrO_3$ thin films

Chih-Yi Liu [a], Chun-Chieh Chuang [a], Jian-Shian Chen [a], Arthur Wang [b], Wen-Yueh Jang [b], Jien-Chen Young [b], Kuang-Yi Chiu [b], Tseung-Yuen Tseng [a,*]

[a] *Department of Electronics Engineering and Institute of Electronics, National Chiao-Tung University, Hsinchu 300, Taiwan*
[b] *Winbond Electronics Corp., Hsinchu 300, Taiwan*

Available online 6 September 2005

Abstract

V-doped $SrZrO_3$ (SZO) thin films on $LaNiO_3/SiO_2/Si$ substrate are synthesized by sol–gel method to form metal–insulator–metal (MIM) sandwich structure. The physical and electrical properties of the MIM device are studied. The structure and surface morphology of the SZO films are also characterized by X-ray diffraction and scanning electron microscopy. Such a device has the bistable switching properties of current–voltage characteristics. The resistive switching between high state and low state can also be operated with voltage pulses. The device with the properties of long retention time and non-destructive readout is expected to be suitable for nonvolatile memory application.
© 2005 Elsevier B.V. All rights reserved.

Keywords: $SrZrO_3$; Memory effect; Nonvolatile memory; RRAM

1. Introduction

Following the popularity of portable equipments, such as mobile phone, digital camera, and notebook computer, nonvolatile memory becomes one of the mainstreams of semiconductor industry. The nonvolatile memory device should keep the stored information for a long time without requiring power supply. The criteria for a perfect nonvolatile memory device include low operation voltage, low power consumption, long retention time, small cell size, high operation speed, low cost, high endurance, non-destructive readout, and simple structure [1]. However, so far there is no nonvolatile memory device that satisfies all these requirements. Although flash memory is the mainstream among the nonvolatile memory devices nowadays, it has many drawbacks including high operation voltage, low operation speed, and poor endurance. In addition, as the device is continuously scaled down in size, the flash memory faces the challenge of gate oxide thinning that causes the unsatisfactory retention time. Therefore, many nonvolatile memories are eagerly investigated to replace flash memory. Resistance random access memory (RRAM) is one of the promising candidates for the next generation nonvolatile memory application. Perovskite materials are investigated for many applications, such as gate dielectrics [2], dynamic random access memory (DRAM) [3], and tunable microwave device [4]. Recently, Beck et al. proposed that Cr-doped $SrZrO_3$ (SZO) film had reversible bistable switching properties and was suitable for nonvolatile memory application [5]. We adopted the oriented $LaNiO_3$ film as the bottom electrode for the considerations of low cost and low process temperature. In this paper, we used the sol–gel method to deposited V-doped SZO films to investigate their electrical and physical properties. Sol–gel method has the advantages that include low cost, easy stoichiometric control, and high uniformity. The influence of process conditions of thermal treatment on the physical properties of the films was also investigated. The V-doped SZO film was found to have the reversible switching behavior and the memory effect.

2. Experimental procedures

The 4-in. boron-doped p-type (100) silicon wafer was adopted as substrate for device fabrication. After the standard Radio Company of America (RCA) cleaning, the

* Corresponding author. Tel.: +886 3 5731879; fax: +886 3 5724361.
E-mail address: tseng@cc.nctu.edu.tw (T.-Y. Tseng).

0040-6090/$ - see front matter © 2005 Elsevier B.V. All rights reserved.
doi:10.1016/j.tsf.2005.08.153

200-nm thick SiO_2 film was thermally grown by a furnace to insulate the leakage current density from Si substrate. Then the 100-nm thick $LaNiO_3$ (LNO) film was deposited at 300 °C by a radio-frequency (rf) magnetron sputter as the bottom electrode. The base pressure of the vacuum chamber was 1.3×10^{-3} Pa. The power density was fixed at 23.3 W/cm^2 and constant working pressure of 5.3 Pa which was maintained by a mixture of Ar and O_2 at a mixing ratio of 3:2 with a total flow of 40 sccm. The deposited LNO film with (100) and (200) preferred orientation was verified by XRD, which is suitable as a template. After that, the 0.2% V-doped $SrZrO_3$ films with 50 nm thickness were prepared by an acetate precursor sol–gel route on the bottom electrode as the resistive layer. Stoichiometric amounts of the starting materials including strontium acetate (ALDRICH, 99.995%), zirconium n-propoxide (ALDRICH, 70 wt.% solution in 1-propanol), and V_2O_5 (MERCK, 99%), were dissolved in acetic acid (FLUKA, 99.8%) and acetylacetone (FLUKA, 99.5%) to form the solution for sol–gel film preparation. The above-prepared 0.1 M precursor solution was spin-coated on the LNO/SiO_2/Si substrates to form sol–gel film. Then the deposited layer was heat-treated at 200 °C for 10 min and then annealed for 30 min. The coating and heating steps were repeated to obtain the desired film thickness. Finally, 300-nm thick Al film with area of 4.9×10^{-4} cm^2 was deposited by a thermal evaporator and then patterned by a metal mask as the top electrode. The thermogravimetry (TG) and the differential thermal analysis (DTA) of the dried gel-form precursor powders were analyzed by Seiko SSC 5000. The thermal analysis was carried out at a heating rate of 10 °C/min and Al_2O_3 was used as the standard material. The structure of SZO films was characterized by X-ray diffraction (XRD, Cu Kα, $\lambda = 0.15405$ nm, 0.02°2θ step, Rigaku DMaxB X-ray diffractometer) and surface morphology was observed by scanning electron microscopy (SEM, Hitachi S4700). The electrical measurements of the MIM device were performed by Agilent 4155 C and 81110 A. The Agilent 81110 A was employed to generate voltage pulses to change the resistance of the device and the Agilent 4155 C was used to measure the leakage current density of the device.

3. Results and discussion

Fig. 1(a) shows the TG and the derivative thermogravimetry (DTG) of the dried gel-form precursor powders. The weight loss obtained from the TG indicates that the organic component of the precursor was decomposed with increasing temperature and pyrolyzed between 400 and 600 °C. Therefore, the organic moieties of the precursor would be completely removed at around 600 °C. As shown in Fig. 1(b), the DTA of the dried gel-form precursor powders indicates that the temperature of end point of the pyrolysis is about 575 °C, which is consistent with the TG results. Fig. 2 shows the XRD patterns of the V-doped SZO films annealed

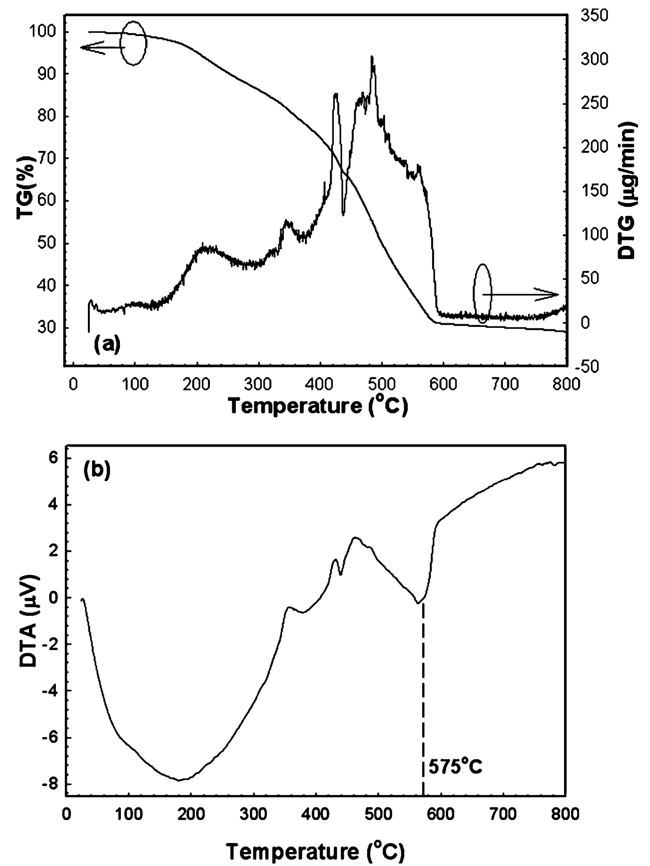

Fig. 1. (a) TG and DTG curves of the dried gel-form precursor; (b) DTA curve of the dried gel-form precursor.

at various temperatures, indicating that the LNO bottom electrodes after thermal process are still oriented to (100) and (200). The values of 2 theta for LNO films increase with increasing annealing temperature, indicating that the lattice constant of LNO films decreases with increasing annealing temperature. In addition, the peaks of SZO films do not appear until the annealing temperature is higher than 600 °C. In other words, the SZO films crystallized above 600 °C, which is consistent with the DTA results (Fig. 1(b)). The SZO films have the (200) preferred orientation, which is the same as that of the LNO bottom electrode. This means that the LNO bottom electrode served as the template to lead the film to form with the same preferred orientation. The V-doped SZO films were annealed at various temperatures. The SZO films annealed at 400 and 600 °C have crack-free uniform and smooth microstructure composed of ultra fine grains (<25 nm) on the basis of SEM observation (not shown here). The 400 °C annealed SZO film still has some residue on the surface. However, the residue was removed from the film with SZO at 600 °C as the annealing temperature. The residue on the surface should be related to the organic impurity in the SZO film. Therefore, higher annealing temperature would remove the surface residue. Fig. 3(a) shows the plot of the leakage current density vs. bias voltage for the device fabricated at 400 °C. Before any change in resistance is caused by the bias voltage, the

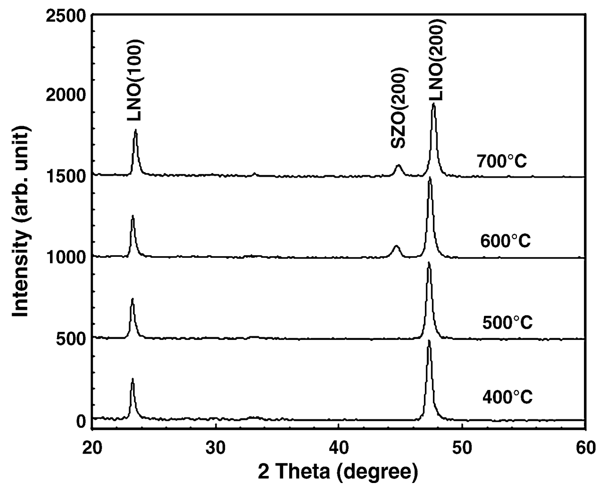

Fig. 2. XRD patterns of V-doped SZO films annealed at various temperatures.

leakage current density increases with increasing bias voltage, which is defined as the original-state. The negative leakage current density increases with increasing negative bias voltage. When the negative bias voltage is higher than −8 V, the leakage current density increases abruptly from the original state to higher leakage current density, which is defined as the high state. The leakage current density of high state increases with increasing positive bias voltage. When the positive bias voltage is higher than +6 V, the leakage current density drops from the high state to lower leakage current density, which is defined as the low state. However, the leakage current density of the low state is larger than that of the original state. While the negative bias voltage is higher than −7 V again, the leakage current density is changed from the low state to the high state. The sequence of resistance switching could be reversibly changed between the high state and the low state, but never back to the original state. The resistance ratio operated by dc bias sweep is about 3 orders of magnitude. The resistance ratio decreases with decreasing bias voltage, which should be due to the different conduction mechanisms of the high state and the low state [6]. There is another interesting phenomenon in Fig. 3(a), where the initial resistance change needs larger voltage. Besides, so far the reason for the polarity of the resistance change is not clear, which needs further studies to clarify this point. As can be seen in Fig. 3(b), the device can also be operated by voltage pulses. After adding a +15 V, 500 μs voltage pulse on the device, the state was switched to low state. Then, adding a −15 V, 500 μs voltage pulse on the device, the low state was changed to high-state. The polarity of the resistance change is the same as that of the bias voltage operation. The resistance ratio operated by voltage pulse is about 3 orders of magnitude. The voltage pulse operation is reversible, which is suitable for practical application. While the cycling number increases, the leakage current density of high state kept almost the same and that of low-state increased gradually. The increase in leakage current density of low state would be due to the increase of trap density. As indicated in Fig. 4, the retention behavior of the device was investigated. In order to avoid the tedious measurement of the retention time of the memory state at room temperature, the thermal acceleration testing was used. The plots of

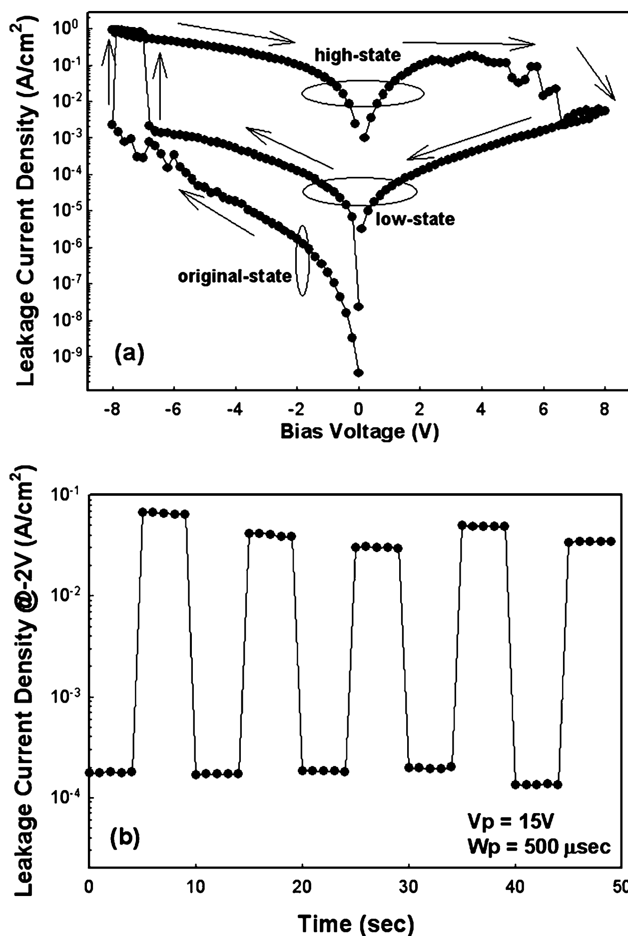

Fig. 3. (a) Plot of leakage current density vs. bias voltage of 400 °C annealed SZO film and (b) plot of leakage current density vs. time by voltage pulse operating of the film.

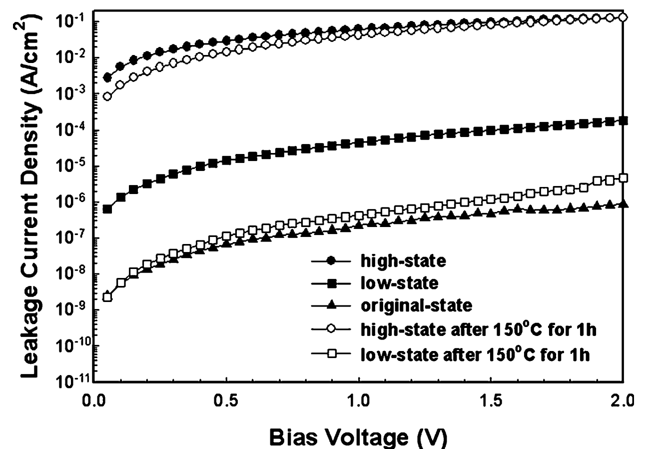

Fig. 4. Plots of leakage current density vs. bias voltage of original state, low state, and high state and those of low state and high state after heating at 150 °C for 1 h.

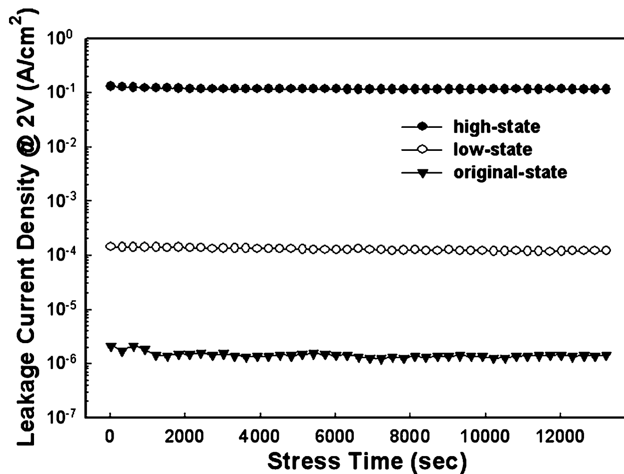

Fig. 5. Plots of leakage current density vs. time for 2 V applied stress.

leakage current density vs. bias voltage for different states and those after thermal acceleration testing are shown in Fig. 4. To prevent oxidation of the Al top electrode, the thermal acceleration testing was performed in N_2 ambient at 150 °C in 1 atm pressure for 1 h. After thermal acceleration, the leakage current density of the high-state was decreased a little and still very close to the previous one. On the other hand, the leakage current density of the low state after thermal acceleration was decreased largely and close to the leakage current density of the original state. For a thermal acceleration with higher temperature, the leakage current density of the high state would also drop to the leakage current density of the original state (not shown here). This phenomenon means that the original-state is the most stable state. The phenomenon of retention behavior of our devices is not similar to other types of memory materials such as the ferroelectric materials. Although the leakage current density of low-state drops faster than that of the high state, it is still good enough to distinguish the two different states. Therefore, it indeed conforms to the need of practical operation. Fig. 5 shows the plots of leakage current density vs. stress time for the different states. The 2 V voltage bias was applied to the device for more than 3 h and the leakage current density of different states does not change. In general, the read time is about several 10 ns and the read amplitude is less than 1 V. Fig. 5 shows the stability of the leakage current density after stressing at 2 V/3 h, indicating that the leakage-states were not varied after the read operation (1 V/10 ns). Therefore, the non-destructive readout property is demonstrated. Furthermore, the criterion of read operation is about 10^{12} times. Therefore, the accumulative time of read operation is about 10^4 s. In addition, the stress voltage adopted was larger than 1 V and the stress time was more than 3 h (Fig. 5). Therefore, the stress testing should be equivalent to the read operation larger than 10^{12} times. Besides, after large current density stresses, the leakage current densities of the device for different states do not increase, indicating that the device has the excellent electrical properties. Our device with the properties of low operation voltage, high operation speed, high resistance ratio, long retention, and non-destructive readout, is expected to be suitable for the next generation nonvolatile memory applications.

4. Conclusions

The sol–gel derived 0.2% V-doped SZO film was deposited on LNO bottom electrode to form MIM structure. The TG and DTA studies of the dried gel-form precursors were carried out to find suitable processing temperature. The XRD and SEM observations of the SZO films with different thermal treatments were performed to understand their structure and surface morphology. The memory effect of Al/SZO/LNO/SiO_2/Si MIM structure was operated by bias voltage and voltage pulse. The state of the device can be distinguished as three states: original-state, low state, and high state. After the initial switching, the leakage current density was only switched between low state and high state. The results of thermal acceleration testing on the device reveal that after testing, the leakage current density of the high state almost keeps the same, however, the leakage current density of the low-state drops very large, which is close to that of the original state. The memory state was not changed after the voltage stress was applied for a long time. Our device has a non-destructive readout property.

Acknowledgement

The authors thank the financial supports from the National Science Council of R.O.C. under project no. NSC 93-2215-E009-048 and the Winbond Electronics Corp., Taiwan.

References

[1] W.W. Zhuang, W. Pan, B.D. Ulrich, J.J. Lee, L. Stecker, A. Burmaster, D.R. Evans, S.T. Hsu, M. Tajiri, A. Shimaoka, K. Inoue, T. Naka, N. Awaya, K. Sakiyama, Y. Wang, S.Q. Liu, N.J. Wu, A. Ignatiev, IEDM Tech. Dig. (2002) 193.
[2] C.Y. Liu, H.T. Lue, T.Y. Tseng, Appl. Phys. Lett. 81 (2002) 4416.
[3] M.S. Tsai, S.C. Sun, T.Y. Tseng, IEEE Trans. Electron Devices 46 (1999) 1829.
[4] H.T. Lue, T.Y. Tseng, IEEE Trans. Ultrason. Ferroelectr. Freq. Control 48 (2001) 1640.
[5] A. Beck, J.G. Bednorz, Ch. Gerber, C. Rosseel, D. Widmer, Appl. Phys. Lett. 77 (2000) 139.
[6] C.Y. Liu, P.H. Wu, A. Wang, W.Y. Jang, J.C. Young, K.Y. Chiu, T.Y. Tseng, IEEE Electron Device Lett. 26 (2005) 351.